Molecular Biology of the Cell
Vol. 21, 2057–2065, June 15, 2010

Peroxisomal Membrane Proteins Insert into the Endoplasmic Reticulum

Adabella van der Zand, Ineke Braakman,* and Henk F. Tabak*

Cellular Protein Chemistry, Faculty of Science, Utrecht University, NL-3584 CH Utrecht, The Netherlands

Submitted February 1, 2010; Revised April 7, 2010; Accepted April 20, 2010
Monitoring Editor: Howard Riezman

We show that a comprehensive set of 16 peroxisomal membrane proteins (PMPs) encompassing all types of membrane topologies first target to the endoplasmic reticulum (ER) in *Saccharomyces cerevisiae*. These PMPs insert into the ER membrane via the protein import complexes Sec61p and Get3p (for tail-anchored proteins). This trafficking pathway is representative for multiplying wild-type cells in which the peroxisome population needs to be maintained, as well as for mutant cells lacking peroxisomes in which new peroxisomes form after complementation with the wild-type version of the mutant gene. PMPs leave the ER in a Pex3p-Pex19p–dependent manner to end up in metabolically active peroxisomes. These results further extend the new concept that peroxisomes derive their basic framework (membrane and membrane proteins) from the ER and imply a new functional role for Pex3p and Pex19p.

INTRODUCTION

Peroxisomes belong to the basic repertoire of organelles in eukaryotic cells. They were first isolated by the group of De Duve, and initial studies focused on the enzymes they contained to understand their contribution to cellular metabolism (De Duve and Baudhuin, 1966). The enzyme content can vary depending on species, explaining why initial description led to different names: peroxisomes, glyoxysomes, and glycosomes. Now, it is clear that these organelles all belong to the same microbody family based on conserved features. For example, the ability to degrade fatty acids as well as the presence of conserved peroxisomal targeting signal (PTS) 1 and PTS2 on enzymes is widespread (Gould *et al*., 1987; Swinkels *et al*., 1992; Gabaldon *et al*., 2006; Schluter *et al*., 2007). Enzymes are imported from the cytosol into peroxisomes by a protein import machinery located in the peroxisomal membrane (importomer) (Rachubinski *et al*., 1984). Particularly, this last feature formed the basis for the proposal that peroxisomes are autonomous organelles that multiply by growth and division (Lazarow and Fujiki, 1985; Subramani, 1998).

New tools for investigating this concept became available when genetic screens were used to isolate mutants with disturbances in peroxisome function. It led to the discovery of Pex proteins with a function in peroxisome formation and maintenance (Erdmann *et al*., 1989; Tsukamoto *et al*., 1990; Elgersma *et al*., 1993; Wanders, 1999; Gould and Valle, 2000). Remarkable representatives were Pex3p and Pex19p, because cells harboring mutant versions of these genes have lost the complete peroxisome population. However, upon reintroduction of a wild-type *PEX3* or *PEX19* gene in such mutants, the peroxisome population is restored even after many generations of growth without peroxisomes (Höhfeld *et al*., 1991). The question arises: where do these new peroxisomes come from?

Already in the early days of peroxisome research there were hints that the endoplasmic reticulum (ER) might be involved. Electron microscopic observations indicated that peroxisomes are often found in close association with the ER (Novikoff and Novikoff, 1972), and pulse-chase experiments using germinating castor beans showed that peroxisomal proteins passed through the ER before they appeared in glyoxysomes (specialized peroxisomes) (González and Beevers, 1976; González, 1986). The Δ*pex3*/Δ*pex19* mutants sparked a new interest in the relationship between ER and peroxisomes, and evidence for an important contribution of the ER to peroxisome formation was mounting.

Pulse-chase analysis in *Yarrowia lipolytica* showed that Pex2p and Pex16p appeared first in the ER, were glycosylated and then accumulated in peroxisomes (Titorenko and Rachubinski, 1998). The ER concept gained further momentum with the discovery, by immunoelectron microscopy in mouse dendritic cells, of Pex13p being present in specialized parts of the ER and in lamellar structures (peroxisomal precompartments) (Geuze *et al*., 2003). In three-dimensional reconstructions, these lamellae were shown to be in continuity with peroxisomes (Tabak *et al*., 2003). The nature and distribution of proteins over these various compartments suggested a developmental pathway starting in the ER and leading to mature peroxisomes. This was further elaborated in *Saccharomyces cerevisiae* whereby the formation of peroxisomes was followed using real-time fluorescence microscopy (Hoepfner *et al*., 2005). Newly synthesized yellow fluorescent protein (YFP)-tagged Pex3p appeared first in the ER and subsequently via preperoxisomal structures in peroxisomes. A similar trafficking route for Pex3p was also reported by others in yeast (Kragt *et al*., 2005; Tam *et al*., 2005; Haan *et al*., 2006; Motley and Hettema, 2007), plants (Karnik and Trelease, 2007), and mammalian cells (Kim *et al*., 2006).

This involvement of the ER could also explain the Δ*pex3*/Δ*pex19* paradox mentioned above: the lost population of peroxisomes can be restocked through the contribution of the ER. But how extensive is this contribution? Here, we show that 16 peroxisomal membrane proteins (PMPs) dis-

This article was published online ahead of print in *MBoC in Press* (http://www.molbiolcell.org/cgi/doi/10.1091/mbc.E10–02–0082) on April 28, 2010.

* These authors contributed equally to this work.

Address correspondence to: Henk F. Tabak (h.f.tabak@uu.nl).

playing all types of membrane topology enter the ER via the Sec61p translocon or the Get3 protein, attain their correct topology, and travel to peroxisomes. Thus, the basic framework for a functional peroxisome, membrane with PMPs, is delivered by the ER, making peroxisomes an intrinsic member of the endomembrane family.

MATERIALS AND METHODS

DNA Manipulations, Cloning Procedures, and Strain Constructions

Yeast strains used in this study are listed in Supplemental Table S1. Polymerase chain reaction (PCR)-based methods were used to construct gene deletion cassettes, cyan fluorescent protein (CFP)/YFP-fusion- or *GAL1*-fusion-cassettes for transformations (Janke *et al*., 2004). Oligonucleotides (oligos) are listed in Supplemental Table S2. DNA of *Escherichia coli* plasmids pFA6-kanMX6; pFA6-HisMX6; pFA6-*kl*TRP1 (Wach *et al*., 1994), pFA6-NatMX (Goldstein and McCusker, 1999), pDH3 and pDH5 (Yeast Resource Center, University of Washington, Seattle, WA), and pFA6-KanMX6-PGAL1-GFP and a pFA6-His3MX6-PGAL1-GFP (Longtine *et al*., 1998) variant with the green fluorescent protein (GFP) exchanged for YFP served as template for preparative PCR reactions. Genomic integration of the corresponding construct was verified by analytical PCR (Wach *et al*., 1994). Plasmid pEW177 containing CFP-PTS1 was constructed as described previously (Hoepfner *et al*., 2001). The *GAL1-PEX3* integration plasmid (*pAZ102*) was constructed by excising the *YFP* open reading frame from pDHsb1 (Hoepfner *et al*., 2005) with XmaI and religation. The *GAL1-PEX8-YFP* integration plasmid (*pTH2*) was constructed as follows: YFP was amplified by PCR from pDH5 using oligonucleotides introducing flanking HindIII and XhoI sites. The fragment was cloned into the corresponding sites of pNB527 (Jiang and Ferro-Novick, 1994), resulting in pTH1. *PEX8* was amplified by PCR from the genomic DNA from strain FY1679 (Winston *et al*., 1995) using oligos that introduced HindIII sites. The fragment was cloned into the corresponding site of pTH1. The *GAL1-PEX13-YFP* integration plasmid (*pEW200*) was constructed as follows: the *GAL1* promoter was amplified by PCR from pFA6a-kanMX6-PGAL1 using oligonucleotides introducing flanking EcoRI and SacI sites (Hoepfner *et al*., 2005). The fragment was cloned into the corresponding sites of Yiplac128 (Gietz and Sugino, 1988). An NH-tagged PEX13-YFP fragment from p20.19 (Elgersma *et al*., 1996) was subcloned into the corresponding SacI and HindIII sites of Yiplac128-PGAL1. The GAL-PEX11-YFP (*pTH9*) integration plasmid was constructed as follows: YFP was amplified by PCR from pDH5 using oligonucleotides introducing flanking HindIII and XhoI sites. The fragment was cloned into the corresponding sites of pNB528 (Jiang and Ferro-Novick, 1994), resulting in pTH5. *PEX11* was amplified by PCR from the genomic DNA from strain FY1679 (Winston *et al*., 1995) using oligos that introduced BamHI and HindIII sites. The fragment was cloned into the corresponding sites of pTH5.

Cellular Fractionation

AZY155 cells were grown in YPD at 30°C. Cells were converted into spheroplasts as described previously (Franzusoff *et al*., 1991). To digest the cell wall, yeast lytic enzyme (derived from *Arthrobacter luteus*, 82,800 U/g; ICN) was used at a final concentration of 1.5 U/1.0 OD_{600} of cells. All subsequent steps were carried out at 4°C. Spheroplasts were harvested, resuspended in lysis buffer (20 mM HEPES, pH 7.4, 50 mM KOAc, 100 mM sorbitol, 1 mM EDTA, 1 mM dithiothreitol [DTT], and 1 mM phenylmethylsulfonyl fluoride [PMSF]) and homogenized by vortexing in presence of 0.5-mm glass beads (Biospec Products, Bartlesville, OK). Cell debris was sedimented at 1000 × *g* for 10 min, and the remaining postnuclear supernatant was centrifuged at 20,000 × *g* for 20 min. The resulting membrane pellet was washed twice and resuspended in membrane storage buffer (MSB) (20 mM HEPES, pH7.4, 50 mM KOAc, 250 mM sorbitol, 1 mM DTT, and 1 mM PMSF). Five OD_{280} units of membranes were treated with 1 M NaCl in MSB for 30 min at 4°C or 125 mM Na_2CO_3, pH 11.5, for 30 min at 4°C. Membrane pellets were reisolated by ultracentrifugation at 132,000 × *g* for 10 min in a TLA120.1 rotor (Beckman Coulter, Fullerton, CA) and resuspended in equal volumes of MSB. Alternatively, resuspended membrane pellets were treated with protease. Typically, 200-μl reactions containing 5 OD_{280} units of membranes (in MSB without PMSF) were incubated with fresh 100 μg/ml proteinase K for 20 min at 30°C in presence or absence of 1% Triton X-100. Samples were cooled on ice for 5 min and 10 mM PMSF was added. Fractions were precipitated using methanol and chloroform (4:1). Equivalent amounts were analyzed on 7.5% SDS-polyacrylamide gel electrophoresis (PAGE), transferred to polyvinylidene difluoride (PVDF) membrane, and analyzed by Western blot and enhanced chemiluminescence (ECL).

Buoyant Density Centrifugation

Yeast cells were grown in YPD, and 1000 OD_{600} units of AZY193 cells were harvested, spheroplasted, and postnuclear supernatants were derived after glass bead homogenization (see above). Postnuclear supernatants were layered on top of a 55% sucrose cushion made up in MSB. Gradients were centrifuged at 237,000 × *g* for 2 h at 4°C (SW41Ti rotor; Beckman Coulter). The recovery of membrane material was confirmed by Western blot with antibodies against Pex13p and Sec63p. The membrane fraction was collected and overlaid with a nonlinear (18–54%) sucrose step-gradient (12 ml) made up in MSB and spun to equilibrium for 16 h at 237,000 × *g* (SW41Ti rotor; Beckman Coulter). Twenty-two fractions (540 μl) were collected starting from the top of the gradient using a micropipette. Fractions were precipitated using methanol and chloroform (4:1). Equivalent amounts were analyzed on 10% SDS-PAGE, transferred to PVDF membrane, and analyzed by Western blot and ECL.

Antibodies and Immunoblot Analysis

Mouse polyclonal anti-GFP antibody 1814460 was purchased from Roche Diagnostics (Indianapolis, IN). Antibodies against Hsp60p (Rospert *et al*., 1994), Pex13p (Elgersma *et al*., 1996), Pex14p (Bottger *et al*., 2000), and Kar2p (Hettema *et al*., 1998) have been described previously. Antisera against Sec61p, Sec62p, Sec63p, Nyv1p, and Sso1p were kindly donated by Dr. C. J. Stirling (University of Manchester, Manchester, United Kingdom), and antisera of Pex12p and Pex15p were kindly donated by Dr. Ralf Erdmann (University of Bochum, Bochum, Germany). Immunoreactive complexes were visualized using anti-rabbit, anti-mouse, or anti-sheep immunoglobulin G-coupled horseradish peroxidase (Jackson ImmunoResearch Laboratories, West Grove, PA) in combination with the ECL system from GE Healthcare (Little Chalfont, Buckinghamshire, United Kingdom). The PVDF membranes were exposed to Kodak MR BioMax films (PerkinElmer Life and Analytical Sciences, Boston, MA) and scanned for image processing using Photoshop (Adobe Systems, Mountain View, CA).

Fluorescence Pulse-Chase Assay

Strains for fluorescence pulse-chase analysis were grown overnight in 10 ml of YP-2% raffinose medium to early log phase at 30°C. The cells were spun down and resuspended in an equal volume of YP-2% galactose for 15–30 min and then washed in phosphate-buffered saline (PBS) (Invitrogen, Carlsbad, CA) and taken up in 20 ml of YP-2% glucose. For microscopy, 500-1000 μl of cells was washed with PBS, and 1 μl was spread on a slide overlaid with a coverslip and used immediately for microscopy.

Microscopy Setup and Image Acquisition

Live cell images were taken using an Axiovert 200M fluorescent microscope (Carl Zeiss, Jena, Germany) fitted with a Plan-Neofluar 100× 1.3 numerical aperture Ph3 ∞-0.17 oil immersion objective lens (Carl Zeiss), a Xenon XBO 75W/2 illuminator, and a CoolSNAP HQ monochrome camera (Photometrics, Tucson, AZ). We acquired one phase contrast image and three *z*-axis planes spaced by 0.8 μm. In each *z*-axis plane we acquired one YFP and one cyan fluorescent protein (CFP) image with up to 5-s exposure times and 100% fluorescence transmission without binning. Separately, the YFP and CFP images from the stack were averaged into a single projection using a maximum intensity algorithm (stack arithmetic: maximum command of MetaMorph, version 5; Molecular Devices, Sunnyvale, CA). The YFP/CFP planes were scaled and converted to 8-bit images. The drastic difference in YFP signal intensity during the galactose induction time courses made it necessary to scale individual time points of a time course differently (as apparent by the intensity differences of the background). The phase-contrast, YFP, and CFP images were overlaid with default color balance settings assigning false-color look-up tables using the Overlay Image command of MetaMorph from the main taskbar. Blue color was applied to the phase-contrast picture, green for the YFP channel, and red for the CFP channel. Images were cropped and assembled into figures using Photoshop CS4 (Adobe Systems). To reduce background intensities, we used the Levels command, and to enhance brightness we applied the Curves command in Photoshop to the whole image by using the RGB channel only. The original images we acquired at a resolution of 72 dpi (1392 × 1046 pixels) and were resized to 300 dpi using Photoshop by reducing the physical size of the original image.

N-*[3-Triethylammoniumpropyl]-4-[*p*-diethylaminophenyl-hexatrienyl]pyridinium Dibromide (FM4-64) Staining*

FM4-64 staining of live yeast cells was performed as described previously (Vida and Emr, 1995).

RESULTS

Trafficking of PMPs in Wild-Type Cells

A group of ~22 PMPs are known to have a function in peroxisome formation and maintenance (Marelli *et al*., 2004). We studied the biogenesis of Pex2p, Pex8p, Pex10p, Pex11p, Pex13p, Pex14p, Pex15p, and Ant1p in wild-type cells by using fluorescence microscopy to investigate whether they

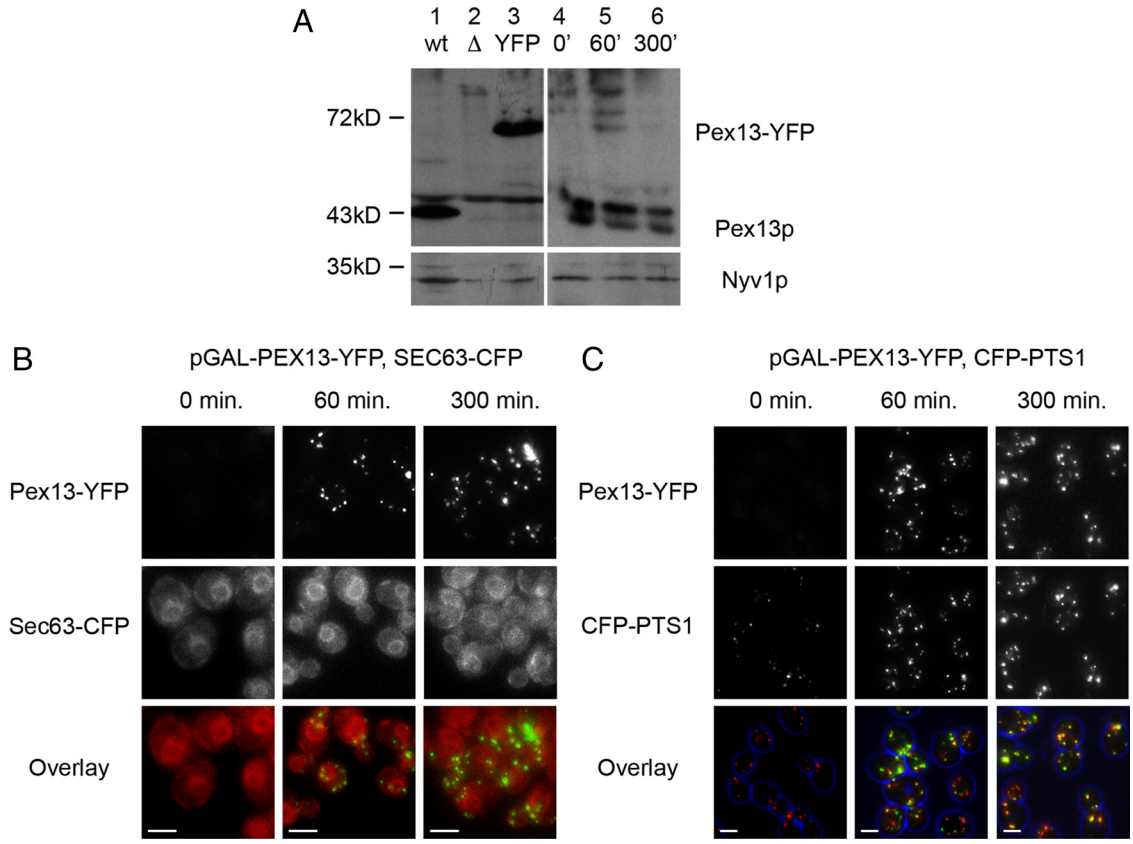

Figure 1. Trafficking of Pex13p in wild-type cells. (A) Cellular Pex13p and Pex13p-YFP levels were measured by loading 2 OD_{600} equivalents of postnuclear supernatants on 10% SDS-PAGE and analysis by immunoblot with antibodies against Pex13p. Lanes 1–3 show glucose grown wild-type (FY1679), Δ*pex13* (AZY258) cells, and wild-type cells expressing Pex13p-YFP from the endogenous promoter (AZY141). Lanes 4–6 show time points of limited expression of *PEX13-YFP* (AZY253) from the *GAL1* promoter. The promoter was induced for 15 min on galactose only, followed by repression on glucose. Samples 4–6 were taken at 0-, 60-, and 300-min glucose chase, respectively. Nyv1p was used as a loading control. (B and C) Fluorescence pulse-chase experiments were performed in wild-type cells. YFP-tagged Pex13p (green) was transiently expressed from the *GAL1* promoter. Peroxisomes were marked with the constitutively expressed CFP-PTS1 (red) (AZY254), whereas the ER was labeled with Sec63p-CFP (red) (AZY253). Sixty minutes after limited expression of *PEX13-YFP* (15-min galactose), the YFP signal localized mostly to ER foci. Wild-type peroxisomes marked with CFP-PTS1 (red) remained largely unlabeled by Pex13p-YFP at this early time point, whereas it colocalized with the ER in cells labeled with Sec63p-CFP. At 300 min, Pex13p-YFP showed complete colocalization with CFP-PTS–containing peroxisomes. Bar, 2 μm.

followed the same trafficking route as Pex3p: inserting first in the ER before ending up in peroxisomes. Pex2p, Pex10p, Pex11p, and Pex13p are polytopic PMPs with two membrane spans and N and C termini facing the cytosol (Okumoto *et al*., 1998; Girzalsky *et al*., 1999; Harano *et al*., 1999; Anton *et al*., 2000), whereas Ant1p (PMP47), which encodes an ATP/ADP translocator, has six membrane spans (McCammon *et al*., 1994). Pex14p is a type I integral membrane protein (Brocard *et al*., 1997) and Pex15p a C-terminally anchored protein (Elgersma *et al*., 1997). Finally, Pex8p, which associates peripherally with the luminal face of the peroxisomal membrane (Agne *et al*., 2003).

PMPs were C-terminally tagged with YFP, put under control of the *GAL1* promoter and integrated into the yeast genome. This allowed us to produce a limited wave of PMP-YFP synthesis comparable with endogenous expression levels. Before induction, cells were grown in raffinose, a medium in which the promoter is on stand-by. PMP synthesis was started by growth in galactose and stopped by repression of the promoter by adding glucose. Using this protocol, we showed before that the amount of Pex3p-YFP that is synthesized corresponds well with the endogenous level and that overproduction is prevented (Hoepfner *et al*., 2005). Here, we show by Western blot analysis that the amount of Pex13p-YFP produced after 15-min galactose induction was less than the level of endogenous Pex13p present (Figure 1A, lanes 4–6). We present the trafficking route of Pex13p as an example using fluorescence pulse-chase experiments. Before induction, no YFP-tagged Pex13p (Figure 1, B and C) was detectable, yet the multipunctate CFP-PTS1 signal indicated the presence of functional peroxisomes (Figure 1C). After induction, Pex13p-YFP first appeared in ER-localized foci that did not colocalize with peroxisomes (Figure 1, B and C). Only later in time, after 300 min, the fluorescent signal of Pex13p-YFP started to coincide with that of peroxisomes (Figure 1C). We found the same route from ER to peroxisomes for other PMPs (Supplemental Figure S1, A–C). Surprisingly, also Pex8p, which needs to translocate across the membrane to reach the lumen, targeted to the ER first (Supplemental Figure S1C). These results demonstrate that in wild-type cells harboring functional CFP-PTS1–containing peroxisomes, the ER is the transit compartment in the trafficking of PMPs to peroxisomes.

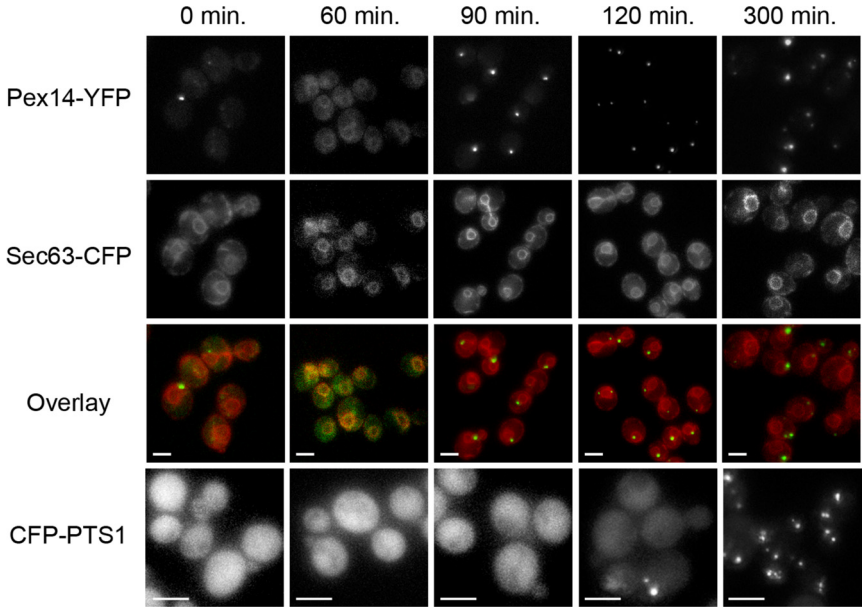

Figure 2. Pex14p trafficking during peroxisome biogenesis in Δ*pex3* cells. Fluorescence pulse-chase experiment in peroxisome-deficient cells. Peroxisome formation is started by short exposure to galactose (30 min) to induce synthesis of Pex3p. Before expression of *PEX3*, most cells displayed no Pex14p-YFP (AZY191). However, a small but significant population of Pex14p-YFP–marked cells showed punctate staining that colocalized with the ER marker Sec63p-CFP (red). Sixty minutes after limited expression of *PEX3*, all cells expressing *PEX14-YFP* showed a weak signal that colocalized with the perinuclear ER (red). At a later stage, Pex14p-YFP started to concentrate into dots frequently localized on or at the periphery of the ER (90 min). At 120 min, Pex14p-YFP localized exclusively to foci mostly no longer overlapping with the Sec63p-CFP signal. At 300 min, the peroxisomal population in the cell has been restored and up to five individual Pex14p-YFP dots per cell were visible. The experiment was also performed in cells expressing CFP-PTS1 to label peroxisomes (AZY192). At the start of the experiment, the exclusively cytosolic CFP-PTS1 demonstrated the absence of import competent peroxisomes (0 min). Despite detectable Pex14p-YFP signal 60–90 min after induction, CFP-PTS1 was uniformly cytosolic, indicating that no import competent peroxisomes had yet been formed. The formation of ER-independent dot-like Pex14p-YFP structures at 120–180 min was accompanied by onset of CFP-PTS1 import, discernible by accumulation of CFP-PTS signal into dots (120 min). At 300 min, the cytosolic background of CFP-PTS1 dropped below detection level and the protein was exclusively peroxisomal, indicating that mature, import-competent peroxisomes have been formed. Bar, 2 μm.

Trafficking of PMPs during Peroxisome Biogenesis

To test additional PMPs more systematically, we used an alternative approach and tagged chromosomal genes encoding 16 different PMPs with YFP at their C-terminal ends with expression driven by their endogenous promoters. These strains all have a Δ*pex3* genetic background with a wild-type *PEX3* gene under the control of the inducible *GAL1* promoter. As a result, these strains have no peroxisomes when grown on raffinose. To induce peroxisome formation in these cells and study the behavior of PMPs, cells were exposed to galactose for 30 min to transiently express Pex3p, followed by glucose to repress the promoter again (Hoepfner *et al*., 2005). We performed the fluorescence pulse-chase assay on the following proteins: Pex1p, Pex2p, Pex3p, Pex4p, Pex6p, Pex8p, Pex10p, Pex11p, Pex12p, Pex13p, Pex14p, Pex15p, Pex19p, Pex25p, Pex27p, and Ant1p. We show results representative for this group.

Pex14p is shown here as an example. Before expression of *PEX3* from the *GAL1* promoter, weak punctate fluorescence of endogenously expressed Pex14p-YFP colocalized with the ER marker Sec63p-CFP (Figure 2, 0 min). Sixty minutes after induction (Figure 2, 60 and 90 min), the additional Pex14p-YFP started to colocalize with the perinuclear ER (Figure 2, 60 min). Later, when the fluorescence signal increased in intensity, Pex14p-YFP appeared at distinct puncta on the ER (Figure 2, 90–120 min) followed by multiple dots, which became independent of the ER (Figure 2, 300 min). Consistent with this is that in the corresponding strain expressing the peroxisomal marker CFP-PTS1 import starts at 120 min and Pex14p-YFP marked puncta colocalized with CFP-PTS1 (Figure 2, bottom). This description is representative for all other PMPs (Supplemental Figure S2, A–D), irrespective of function and membrane topology.

Membrane Topology of PMPs in the ER

To confirm the fluorescence microscopy results, we studied the membrane topology of PMPs using biochemical techniques. PMPs were expressed from their endogenous promoters in *PEX19*-deleted cells (the Δ*pex19* phenotype is identical to the Δ*pex3* phenotype: both lack peroxisomes; Hettema *et al*., 2000). In both mutant cells, PMP-YFP proteins accumulate either in the perinuclear ER or in an ER-localized dot (specialized ER) (Supplemental Figure S3). Homogenates of Δ*pex19* cells were enriched in an organellar fraction, which was analyzed by buoyant density centrifugation in nonlinear sucrose gradients. Immunoblot analysis of the fractions demonstrated that all PMPs equilibrated at the same density (1.192 g/cm^3) coinciding with the first ER peak, indicated by the ER markers Kar2p and Sec63p (Figure 3A). The vacuolar membrane protein Nyv1p, the plasma membrane protein Sso1p and mitochondrial Hsp60p were found to peak at lighter densities. This demonstrates that PMPs localize to the ER, confirming our fluorescence microscopic data in Figures 1 and 2.

We next studied the topology of three different PMPs that form part of the peroxisomal importomer complex: Pex8p, Pex13p, and Pex14p when they are present in the ER (in Δ*pex19* cells). All three proteins fractionated completely into a crude organellar pellet (Figure 3B, lane P), also upon disruption of protein–protein interactions by treating the membrane fractions with 1 M NaCl (Figure 3B, lane NP). However, after treatment at alkaline pH, which converts vesicles into membrane sheets, Pex8p-YFP, like Kar2p, fractionated into the supernatant fraction consistent with it being a luminal protein (Figure 3B, lane CS). Pex13p and Pex14p, as integral membrane proteins, cofractionated together with Sec63p-CFP in the pellet fraction (Figure 3B, lane CP). The crude organellar pellet fraction was also treated with proteinase K. Pex8p-YFP and Kar2p remained fully protected against protease and only degraded after addition of detergent (Figure 3B, lanes PK and PK + Triton X-100 [TX100]). The cytosolically faced SH3 epitope of Pex13p was degraded upon proteinase K treatment, as well as Pex14p. The experiment was controlled using Kar2p as luminal and

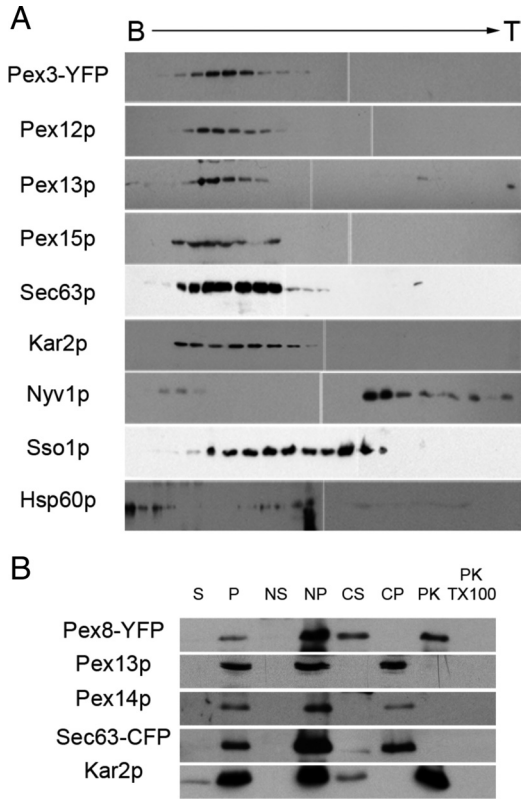

Figure 3. Insertion and maturation of PMPs into the ER. (A) Organellar fraction of a Δ*pex19* homogenate (AZY193) was subjected to buoyant density centrifugation on nonlinear sucrose step gradients to confirm ER localization of PMPs. Fractions were collected from top (T) to the bottom (B) and analyzed by Western blot with indicated antibodies. (B) Postnuclear supernatants prepared from AZY155 cells were fractionated into supernatant (S) and membrane pellet (P) fractions. Pellet fractions were extracted with NaCl or Na_2CO_3 (pH 11.5) and reisolated to generate salt supernatant (NS), salt pellet (NP), carbonate supernatant (CS), and carbonate pellet (CP), or the pellet fractions were treated with proteinase K (PK) or proteinase K with 1% Triton X-100 (PK TX100).

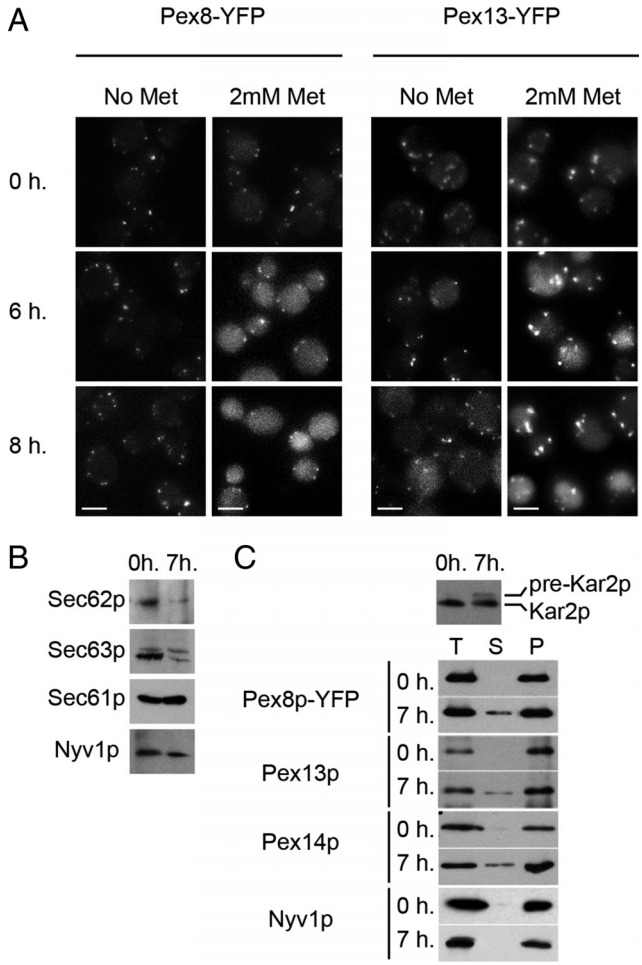

Figure 4. Translocation of PMPs is dependent on the classical ER import machinery. (A) Cells expressing methionine-regulated *SEC62* and *SEC63* (BYY12) and chromosomally tagged *PEX8-YFP* (AZY250) or *PEX13-YFP* (AZY289) were used to test the contribution of the Sec61p translocon to PMP insertion. Unrepressed (0 h) cells expressing *SEC62* and *SEC63* contained multiple Pex8p-YFP or Pex13p-YFP puncta representing peroxisomes. Six to 8 h after addition of 2 mM methionine (Met), both Pex8p- and Pex13p-YFP started to accumulate diffusely in the cytosol, and the number of YFP fluorescent puncta decreased compared with untreated cells. Bar, 2 μm. (B) BYY12 cells were grown for 7 h in the absence or presence of 2 mM methionine to deplete the cells of Sec62p and Sec63p. Two OD_{600} equivalents of postnuclear supernatants were prepared and separated by 10% SDS–PAGE before analysis by immunoblotting with antibodies specific to Sec61p, Sec62p, and Sec63p. Nyv1p was used as a loading control. (C) *SEC62/SEC63* shutoff cells expressing *PEX8-YFP* in a Δ*pex3* background (AZY249) were grown in the presence or absence of 2 mM Met for 7 h, and cell extracts were prepared. Both ER-translocated Kar2p (signal peptide cleaved) and untranslocated (cytosolic) precursor form of Kar2p (preKar2p) are indicated. Postnuclear supernatants were harvested (T) and subsequently fractionated into supernatant (S) and membrane pellet (P) fractions. Western blot analysis was performed on these fractions with the indicated antibodies.

Sec63p-CFP as membrane marker of the ER (Sec63p-CFP is protease sensitive because we monitored the behavior of the CFP tail, which extends into the cytosol). Together, these experiments illustrate that PMPs in Δ*pex19* cells are present in the ER and attain their properly folded state and polarity in the membrane. An implication of these findings is that Pex3p and Pex19p are not essential for the recognition and membrane insertion of newly synthesized PMPs into the peroxisomal membrane but are necessary for exit from the ER.

Insertion of PMPs via the ER-specific Translocons

We next studied whether the Sec61p complex supported the entry of PMPs into the ER, because the majority of proteins entering the ER do so via the essential Sec61p complex. We therefore gradually depleted cells of their capacity to import proteins into the ER. Wild-type cells were used to replace both endogenous promoters of *SEC62* and *SEC63* with the repressible *MET3* promoter (Young *et al*., 2001) and chromosomally expressed *PEX8* or *PEX13* tagged with YFP at the C terminus. Expression of these PMPs is driven from their corresponding endogenous promoters. Addition of methionine to the growth medium shuts down the *MET3* promoter. This results in depletion of the essential Sec proteins and decreases the protein import capacity via both co- and post-translational translocation into the ER (Young *et al*., 2001).

For fluorescence microscopy, cells were grown in the presence or absence of methionine, and images were acquired at different time points. At 0 min, both Pex8p-YFP and Pex13p-YFP were present in several fluorescent foci, demonstrating

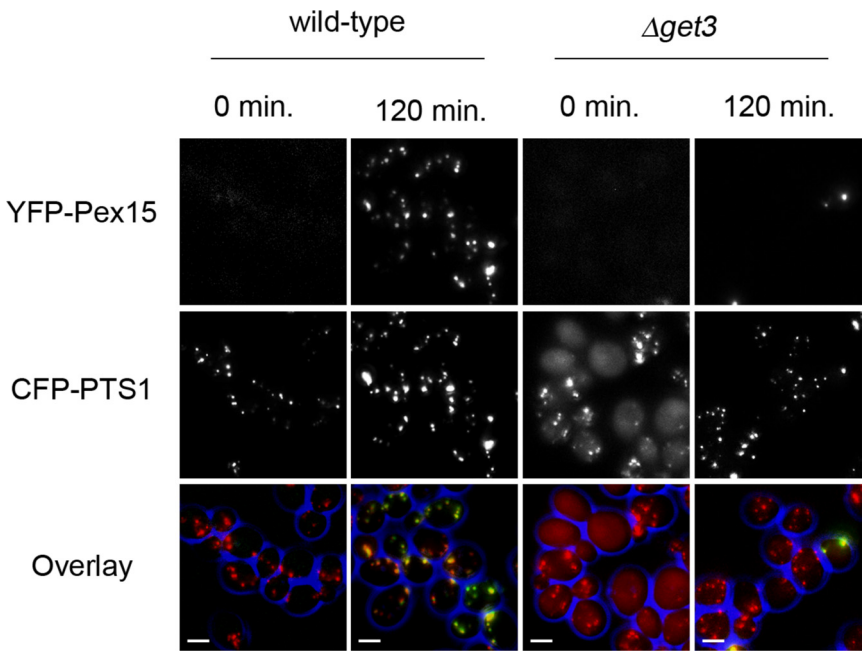

Figure 5. Translocation of Pex15p is dependent on Get3p. Chromosomally YFP-tagged *PEX15* was placed under control of the *GAL1* promoter and expressed in wild-type (AZY299) or in *GET3* deleted (AZY278) cells for use in fluorescent pulse-chase experiments. Within 120 min after limited expression of *YFP-PEX15* (15 min galactose treatment), YFP fluorescence (green) colocalized with CFP-PTS1–labeled peroxisomes (red) in wild-type cells. In Δ*get3* cells, CFP-PTS1 was predominantly cytosolic before induction. CFP-PTS1 import was rescued by limited expression of *YFP-PEX15*. However, the YFP-Pex15p signal itself remained largely undetectable and failed to reach peroxisomes in the Δ*get3* cells. Bar, 2 μm.

their specific localization to peroxisomes (Figure 4A). Six to 8 h after addition of methionine, part of the YFP fluorescence became diffuse, indicating that both Pex8p-YFP and Pex13p-YFP were accumulating in the cytosol (Figure 4A). During this experiment, we also monitored the amount of essential Sec proteins by using Western blotting. Cells were grown in the presence or absence of methionine, and total cell extracts were prepared. Seven hours after shutoff, the levels of Sec62p and Sec63p became significantly reduced but not completely depleted, whereas the levels of Sec61p remained unaffected (Figure 4B). We confirmed these results using biochemical fractionation combined with Western blotting. To avoid the problem of the possibility of leakage from peroxisomes contaminating the supernatant fraction, we performed the cellular fractionation experiments in Δ*pex3* cells that lack peroxisomes, and we blotted for various PMPs. As a positive control for ER translocation capacity we used Kar2p, which uses both co- and posttranslational translocation routes (Ng *et al*., 1996). Like the fluorescence microscopy results, the translocation defect emerged 7 h after shutoff, as indicated by the appearance of the slower migrating precursor form of Kar2p in addition to the mature luminal form (Figure 4C). (Kar2p is not glycosylated and the lower mobility of the precursor form represents the presence of an uncleaved signal sequence.) The majority of Kar2p was processed (Figure 4C), indicating that despite the decrease in import the ER remained fully stocked with resident proteins (Figure 4B), thus minimizing the risk of indirect effects on PMP import into the ER.

Pex8p-YFP, Pex13p, and Pex14p were expressed from their corresponding endogenous promoters and cosedimented in the pellet fraction in cells without methionine repression (Figure 4C, lane P, 0 h). Yet, 7 h after Sec62p and Sec63p depletion, PMPs showed a translocation defect reflected in a significant pool of untranslocated, soluble protein (Figure 4C, lane S, 7 h). To verify the specificity of the Sec62p/Sec63p depletion, we studied the behavior of the tail-anchored protein Nyv1p, a vacuolar vesicle-soluble *N*-ethylmaleimide-sensitive factor attachment protein receptor (v-SNARE). Tail-anchored proteins translocate independently of the Sec61p translocon into the ER (Steel *et al*., 2002). Indeed, Nyv1p was stably integrated under all conditions tested, and there was no evidence of a soluble pool of Nyv1p (Figure 4C). In addition, this control indicates that the ER remains functional during the depletion period. Together, the Western blot data and microscopy results shown for several topologically distinct PMPs suggest the involvement of the general protein import machinery (the Sec61p complex) for PMP import into the ER.

Recently, a dedicated protein translocation machinery has been identified that is specific for delivering and inserting tail-anchored proteins into the ER membrane. This novel ATP-dependent pathway requires the contribution of the cytosolic protein Asna-1/TRC40 in mammalian cells (Stefanovic and Hedge, 2007) or Get3p in yeast (Schuldiner *et al*., 2008). Because peroxisomal Pex15p is a tail-anchored protein (Elgersma *et al*., 1997), which was shown to interact with Get3p via its transmembrane domain (Schuldiner *et al*., 2008), we tested the effect of deleting *GET3* on ER targeting of Pex15p in a fluorescent pulse chase. Wild-type and Δ*get3* cells were used in which the chromosomal copy of *PEX15* was replaced for *YFP-PEX15* under control of the *GAL1* promoter. In addition, cells expressed CFP-PTS1 to report the presence of protein import competent peroxisomes.

In wild-type cells, no YFP fluorescence was observed before induction of YFP-Pex15p (Figure 5, 0 min); however, the punctate pattern of CFP-PTS1 indicates the presence of some peroxisomes. In wild-type cells, YFP-Pex15p fluorescence colocalized with CFP-PTS1–marked peroxisomes 120 min after a short period of YFP-Pex15p synthesis (15 min galactose pulse followed by glucose chase) (Figure 5, 120 min). Conversely, in most Δ*get3* cells, YFP-Pex15p levels did not rise above detection level after a 15-min galactose induction (Figure 5, 120 min). Yet, CFP-PTS1–labeled peroxisomes showed a clear phenotype of the Δ*get3* deletion. Before expression of *YFP-PEX15*, part of the CFP-PTS1 remained cytosolic and part was punctate (Figure 5, 0 min). After induction, the elevated level of YFP-Pex15p suppressed the Δ*get3* phenotype, and all cells had recovered form their peroxisome deficiency (Figure 5, 120 min). The trafficking

block imposed by deleting *GET3* is apparently not tight enough to prevent insertion of YFP-Pex15p and prevent maintenance of some functional peroxisomes. Nonetheless, these results demonstrate that deletion of *GET3* has a profound effect on the kinetics of peroxisomal delivery of Pex15p and formation of peroxisomes, indicating that Pex15p, too, is taken up by an ER-specific protein import machinery. Our data suggest that when import of Pex15p into the ER becomes rate limiting (as in Δ*get3* cells), it cannot bypass the ER and insert into peroxisomes directly, because peroxisomally localized YFP-Pex15p never recovered fully in Δ*get3* cells. Probably, the pool of untranslocated YFP-Pex15p was quickly degraded in the cytosol.

To confirm that the phenotype of the *GET3* deletion is specific to ER-targeted tail-anchored proteins only, we performed fluorescence pulse-chase analyses in Δ*get3* cells of similar genetic design as described above, with the vacuolar tail-anchored protein Nyv1p and with the non-tail-anchored (polytopic) PMP Pex13p. YFP-Nyv1p accumulated in the cytosol in Δ*get3* cells compared with the wild-type control (Supplemental Figure S4A, 120 min). Insufficient Nyv1p targeting to the vacuole leads to a vacuolar fusion defect, which can be visualized by allowing cells to take up the styryl dye FM4-64. Wild-type cells indeed showed fragmented vacuoles before expression of *YFP-NYV1* from the *GAL1* promoter (Supplemental Figure S4A, 0 min). After 30 min of galactose induced synthesis of YFP-Nyv1p, wild-type cells recovered and showed large fused vacuoles, whereas in the *GET3*-deleted strain vacuoles remained smaller and more fragmented (Supplemental Figure S4A, 120 min). In contrast, the nontail-anchored protein Pex13p-YFP appeared in CFP-PTS1–labeled peroxisomes in Δ*get3* cells (Supplemental Figure S4B, 120 min), identical to its localization in wild-type cells. The only difference we observed was a difference in the number of peroxisomes between wild-type and Δ*get3* cells, probably due to defective insertion of Pex15p because deletion of *PEX15* stalls peroxisome development. In accordance with the data published in Schuldiner *et al*. (2008), our results support the notion that Get3p contributes to insertion of tail-anchored proteins of different organellar destination into the ER and that Pex15p makes use of this pathway.

DISCUSSION

Import of PMPs into the ER

A contribution of the ER to peroxisome biogenesis was demonstrated recently, as proof of principle, by way of trafficking of the peroxisomal membrane protein Pex3p in various yeast (Hoepfner *et al*., 2005; Kragt *et al*., 2005; Tam *et al*., 2005; Haan *et al*., 2006) and Pex16p in mammalian and plant cells (Kim *et al*., 2006; Karnik and Trelease, 2007). The question remained how extensive this involvement of the ER is and how this new concept impacts on current ideas about peroxisome formation and maintenance.

We have studied the biogenesis of a representative set of 16 peroxisomal membrane proteins differing in function and membrane topology. We showed by fluorescence pulse-chase analysis that all these proteins first target to the ER before arriving in peroxisomes. We used two genetically different contexts: wild-type cells, where peroxisomes are already present and a Δ*pex3* or a Δ*pex19* mutant in which the full complement of peroxisomes needs to be restored. Biochemical fractionation combined with equilibrium density gradient analysis confirmed that PMPs locate first to the ER. Differential carbonate extraction and protease protection assays demonstrated that the proteins translocate properly into the ER and attain the same topology as described when they are present in the peroxisomal membrane. Extrapolating from this representative set of proteins, we conclude that peroxisomal membrane proteins in *S. cerevisiae* as a rule enter the ER. They subsequently leave the ER in preperoxisomal structures at distinct exit sites. The precompartments are uncoupled from the ER and become competent to import PTS1/PTS2-containing enzymes, forming a new metabolically active peroxisome. Subsequent fission events supported by the dynamins Vps1p and/or Dnm1p keep the number of peroxisomes constant in growing cells (Hoepfner *et al*., 2001; Kuravi *et al*., 2006; Motley and Hettema, 2007; Motley *et al*., 2008). Because peroxisomal fission cannot go on indefinitely, peroxisome numbers can only be maintained through constant supply of ER-derived preperoxisomal structures.

This view is not commonly shared, and authors state that the ER-mediated pathway only comes into play when peroxisomes need to be reformed in mutant cells (Motley and Hettema, 2007). We consider the notion that two distinct mechanisms exist for the formation of peroxisomes, one mechanism in wild-type cells and the other mechanism in mutant cells, unlikely for the following reasons. First, we have experimentally shown here that one and the same principle for peroxisome formation is followed in wild-type and mutant cells. Second, why would single *pex* mutants be found if a separate backup mechanism would exist. Third, this so-called backup system will be called into action rarely and only when a mutation in a particular *PEX* gene occurs that is subsequently restored or compensated for in some other way, again a very rare event. When a biological process is almost never called into operation, it is nearly impossible to keep it functional. The most plausible hypothesis therefore is that one and the same process of peroxisome formation operates in wild-type as well as in mutant cells.

Involvement of ER Protein Import Complexes

The topological variety of PMPs requires the cooperation of different ER-specific translocons. We showed that the general-purpose ER import complex, the Sec61p translocon, is involved. Based on this proof of principle, we consider it likely that other PMPs follow the same route. Application of the SignalP 3.0 algorithm (Bendtsen *et al*., 2004) did not reveal probable signal peptide or signal anchor sequences, nor did we observe telltale marks of protein processing. Thus, the signal(s) that target PMPs to the ER remain to be found.

An exception is the group of tail-anchored proteins, such as Pex15p, which are not inserted via the Sec61p complex. We found that deletion of the tail-anchor protein-specific chaperone encoding *GET3* caused a severe delay in the ER insertion of Pex15p. Surprisingly, the knockout mutant of *GET3* remained viable (Schuldiner *et al*., 2008). This explains why some peroxisomes are still present in the Δ*get3* mutant.

Implications

Our findings that protein import complexes of the ER take care of uptake of PMPs into this compartment disagree with the view on insertion of PMPs into membranes. A current model implicates Pex3p and Pex19p in the direct insertion of peroxisomal proteins from the cytosol into the peroxisomal membrane (Fang *et al*., 2004; Jones *et al*., 2004; Fujiki *et al*., 2006; Matsuzono and Fujiki, 2006). It proposes that Pex19p acts as a chaperone (Jones *et al*., 2004) for newly synthesized PMPs, binding them at a consensus amino acid sequence (mPTS) (Rottensteiner *et al*., 2004) for delivery to the peroxisomal membrane. Interaction between Pex19p and Pex3p

then would lead to the insertion of PMPs into peroxisomal membranes (Fang *et al*., 2004). Our data argue instead for a role of Pex3p and Pex19p in ER budding of the peroxisomal precompartment from the ER, whereby the mPTS may provide a signature for the ER to sort peroxisome-specific cargo from ER resident proteins, to enable specific exit from the ER at distinct sites.

Here, we illustrate that the ER forms an obligate requirement to sustain peroxisomal maintenance in multiplying cells. It is therefore legitimate to view peroxisomes as a specialized subcompartment of the eukaryotic endomembrane system.

Our results confirm new ideas on the evolutionary past of these organelles. Phylogenetic analysis of the peroxisomal proteome showed that the common core of the microbody family consists of Pex proteins and proteins involved in fatty acid metabolism (Gabaldon *et al*., 2006; Schlüter *et al*., 2007). Moreover, some of the oldest Pex proteins are homologous to proteins of the endoplasmic reticulum associated degradation pathway. It all fits well into a concept in which peroxisomes developed from the protoendomembrane system in an early pre-eukaryote (Tabak *et al*., 2006; Cavalier-Smith, 2009).

ACKNOWLEDGMENTS

We thank Dr. Colin Stirling (University of Manchester, Manchester, United Kingdom) and Dr. Ralf Erdmann (University of Bochum, Bochum, Germany) for providing strains and antisera. We thank Danny Schildknegt for contribution and all members of the Braakman laboratory for stimulating discussions. This work was supported by grants from the Academic Biomedical Center of Utrecht University and Nederlandse Organisatie voor Wetenschappelijk Onderzoek-ALW.

REFERENCES

Agne, B., Meindl, N. M., Niederhoff, K., Einwachter, H., Rehling, P., Sickmann, A., Meyer, H. E., Girzalsky, W., and Kunau, W. H. (2003). Pex8p: an intraperoxisomal organizer of the peroxisomal import machinery. Mol. Cell *11*, 635–646.

Anton, M., Passreiter, M., Lay, D., Thai, T. P., Gorgas, K., and Just, W. W. (2000). ARF- and coatomer-mediated peroxisomal vesiculation. Cell Biochem. Biophys. *32*, 27–36.

Bendtsen, J. D., Nielsen, H., von Heijne, G., and Brunak, S. (2004). Improved prediction of signal peptides: SignalP 3.0. J. Mol. Biol. *340*, 783–795.

Bottger, G., Barnett, P., Klein, A. T., Kragt, A., Tabak, H. F., and Distel, B. (2000). Saccharomyces cerevisiae PTS1 receptor Pex5p interacts with the SH3 domain of the peroxisomal membrane protein Pex13p in an unconventional, non-PXXP-related manner. Mol. Biol. Cell *11*, 3963–3976.

Brocard, C., Lametschwandtner, G., Koudelka, R., and Hartig, A. (1997). Pex14p is a member of the protein linkage map of Pex5p. EMBO J. *16*, 5491–5500.

Cavalier-Smith, T. (2009). Predation and eukaryote cell origins: a coevolutionary perspective. Int. J. Biochem. Cell Biol. *41*, 307–322.

De Duve, C., and Baudhuin, P. (1966). Peroxisomes (microbodies and related particles). Physiol. Rev. *46*, 323–357.

Elgersma, Y., van den, B. M., Tabak, H. F., and Distel, B. (1993). An efficient positive selection procedure for the isolation of peroxisomal import and peroxisome assembly mutants of *Saccharomyces cerevisiae*. Genetics *135*, 731–740.

Elgersma, Y., Kwast, L., Klein, A., Voorn-Brouwer, T., van den Beg, M., Metzig, B., America, T., Tabak, H. F., and Distel, B. (1996). The SH3 domain of the *Saccharomyces cerevisiae* peroxisomal membrane protein Pex13p functions as a docking site for Pex5p, a mobile receptor for the import PTS1-containing proteins. J. Cell Biol. *135*, 97–109.

Elgersma, Y., Kwast, L., van den, B. M., Snyder, W. B., Distel, B., Subramani, S., and Tabak, H. F. (1997). Overexpression of Pex15p, a phosphorylated peroxisomal integral membrane protein required for peroxisome assembly in *S. cerevisiae*, causes proliferation of the endoplasmic reticulum membrane. EMBO J. *16*, 7326–7341.

Erdmann, R., Veenhuis, M., Mertens, D., and Kunau, W. H. (1989). Isolation of peroxisome-deficient mutants of *Saccharomyces cerevisiae*. Proc. Natl. Acad. Sci. USA *86*, 5419–5423.

Fang, Y., Morrell, J. C., Jones, J. M., and Gould, S. J. (2004). PEX3 functions as a PEX19 docking factor in the import of class I peroxisomal membrane proteins. J. Cell Biol. *164*, 863–875.

Franzusoff, A., Rothblatt, J., and Schekman, R. (1991). Analysis of polypeptide transit through yeast secretory pathway. Methods Enzymol. *194*, 662–674.

Fujiki, Y., Matsuzono, Y., Matsuzaki, T., and Fransen, M. (2006). Import of peroxisomal membrane proteins: the interplay of Pex3p- and Pex19p-mediated interactions. Biochim. Biophys. Acta *1763*, 1639–1646.

Gabaldon, T., Snel, B., van Zimmeren, F., Hemrika, W., Tabak, H., and Huynen, M. A. (2006). Origin and evolution of the peroxisomal proteome. Biol. Direct. *1*, 8.

Geuze, H. J., Murk, J. L., Stroobants, A. K., Griffith, J. M., Kleijmeer, M. J., Koster, A. J., Verkleij, A. J., Distel, B., and Tabak, H. F. (2003). Involvement of the endoplasmic reticulum in peroxisome formation. Mol. Biol. Cell *14*, 2900–2907.

Gietz, R. D., and Sugino, A. (1988). New yeast-*Escherichia coli* shuttle vectors constructed with in vitro mutagenized yeast genes lacking six-base pair restriction sites. Gene *74*, 527–534.

Girzalsky, W., Rehling, P., Stein, K., Kipper, J., Blank, L., Kunau, W. H., and Erdmann, R. (1999). Involvement of Pex13p in Pex14p localization and peroxisomal targeting signal 2-dependent protein import into peroxisomes. J. Cell Biol. *144*, 1151–1162.

Goldstein, A. L., and McCusker, J. H. (1999). Three new dominant drug resistance cassettes for gene disruption in *Saccharomyces cerevisiae*. Yeast *15*, 1541–1553.

González, E. (1986). Glycoproteins in the matrix of glyoxysomes in endosperm of castor bean seedlings. Plant Physiol. *80*, 950–955.

González, E., and Beevers, H. (1976). Role of the endoplasmic reticulum in glyoxysome formation in castor bean endosperm. Plant Physiol. *57*, 406–409.

Gould, S. G., Keller, G. A., and Subramani, S. (1987). Identification of a peroxisomal targeting signal at the carboxy terminus of firefly luciferase. J. Cell Biol. *105*, 2923–2931.

Gould, S. J., and Valle, D. (2000). Peroxisome biogenesis disorders: genetics and cell biology. Trends Genet. *16*, 340–345.

Haan, G. J., Baerends, R. J., Krikken, A. M., Otzen, M., Veenhuis, M., and van der Klei, I. (2006). Reassembly of peroxisomes in *Hansenula polymorpha* pex3 cells on reintroduction of Pex3p involves the nuclear envelope. FEMS Yeast Res. *6*, 186–194.

Harano, T., Shimizu, N., Otera, H., and Fujiki, Y. (1999). Transmembrane topology of the peroxin, Pex2p, an essential component for the peroxisome assembly. J. Biochem. *125*, 1168–1174.

Hettema, E. H., Ruigrok, C. C., Koerkamp, M. G., van den Berg, M., Tabak, H. F., Distel, B., Braakman, I. (1998). The cytosolic DnaJ-like protein djp1p is involved specifically in peroxisomal protein import. J. Cell Biol. *142*, 421–434.

Hettema, E. H., Girzalsky, W., van den Berg, M., Erdmann, R., and Distel, B. (2000). Saccharomyces cerevisiae pex3p and pex19p are required for proper localization and stability of peroxisomal membrane proteins. EMBO J. *19*, 223–233.

Hoepfner, D., van den Berg, M., Philippsen, P., Tabak, H. F., and Hettema, E. H. (2001). A role for Vps1p, actin, and the Myo2p motor in peroxisome abundance and inheritance in *Saccharomyces cerevisiae*. J. Cell Biol. *155*, 979–990.

Hoepfner, D., Schildknegt, D., Braakman, I., Philippsen, P., and Tabak, H. F. (2005). Contribution of the endoplasmic reticulum to peroxisome formation. Cell *122*, 85–95.

Höhfeld, J., Veenhuis, M., and Kunau, W. H. (1991). PAS3, a *Saccharomyces cerevisiae* gene encoding a peroxisomal integral membrane protein essential for peroxisome biogenesis. J. Cell Biol. *114*, 1167–1178.

Janke, C., *et al*. (2004). A versatile toolbox for PCR-based tagging of yeast genes: new fluorescent proteins, more markers and promoter substitution cassettes. Yeast *21*, 947–962.

Jiang, Y., and Ferro-Novick, S. (1994). Identification of yeast component A: reconstitution of the geranylgeranyltransferase that modifies Ypt1p and Sec4p. Proc. Natl. Acad. Sci. USA *91*, 4377–4381.

Jones, J. M., Morrell, J. C., and Gould, S. J. (2004). PEX19 is a predominantly cytosolic chaperone and import receptor for class 1 peroxisomal membrane proteins. J. Cell Biol. *164*, 57–67.

Karnik, S. K., and Trelease, R. N. (2007). Arabidopsis peroxin 16 trafficks through the ER and an intermediate compartment to pre-existing peroxisomes via overlapping molecular targeting signals. J. Exp. Bot. *58*, 1677–1693.

Kim, P. K., Mullen, R. T., Schumann, U., and Lippincott-Schwartz, J. (2006). The origin and maintenance of mammalian peroxisomes involves a de novo PEX16-dependent pathway from the ER. J. Cell Biol. *173*, 521–532.

Kragt, A., Voorn-Brouwer, T., van den Berg, M., and Distel, B. (2005). Endoplasmic reticulum-directed Pex3p routes to peroxisomes and restores peroxisome formation in a *Saccharomyces cerevisiae* pex3Delta strain. J. Biol. Chem. *280*, 34350–34357.

Kuravi, K., Nagotu, S., Krikken, A. M., Sjollema, K., Deckers, M., Erdmann, R., Veenhuis, M., and van der Klei, I. (2006). Dynamin-related proteins Vps1p and Dnm1p control peroxisome abundance in *Saccharomyces cerevisiae*. J. Cell Sci. *119*, 3994–4001.

Lazarow, P. B., and Fujiki, Y. (1985). Biogenesis of peroxisomes. Annu. Rev. Cell Biol. *1*, 489–530.

Longtine, M. S., McKenzie, A., III, Demarini, D. J., Shah, N. G., Wach, A., Brachat, A., Philippsen, P., and Pringle, J. R. (1998). Additional modules for versatile and economical PCR-based gene deletion and modification in *Saccharomyces cerevisiae*. Yeast *14*, 953–961.

Marelli, M., *et al*. (2004). Quantitative mass spectrometry reveals a role for the GTPase Rho1p in actin organization on the peroxisome membrane. J. Cell Biol. *167*, 1099–1112.

Matsuzono, Y., and Fujiki, Y. (2006). In vitro transport of membrane proteins to peroxisomes by shuttling receptor Pex19p. J. Biol. Chem. *281*, 36–42.

McCammon, M. T., McNew, J. A., Willy, P. J., and Goodman, J. M. (1994). An internal region of the peroxisomal membrane protein PMP47 is essential for sorting to peroxisomes. J. Cell Biol. *124*, 915–925.

Motley, A. M., and Hettema, E. H. (2007). Yeast peroxisomes multiply by growth and division. J. Cell Biol. *178*, 399–410.

Motley, A. M., Ward, G. P., and Hettema, E. H. (2008). Dnm1p-dependent peroxisome fission requires Caf4p, Mdv1p and Fis1p. J. Cell Sci. *121*, 1633–1640.

Ng, D. T., Brown, J. D., and Walter, P. (1996). Signal sequences specify the targeting route to the endoplasmic reticulum membrane. J. Cell Biol. *134*, 269–278.

Novikoff, P. M., and Novikoff, A. B. (1972). Peroxisomes in absorptive cells of mammalian small intestine. J. Cell Biol. *53*, 532–560.

Okumoto, K., Itoh, R., Shimozawa, N., Suzuki, Y., Tamura, S., Kondo, N., and Fujiki, Y. (1998). Mutations in PEX10 is the cause of Zellweger peroxisome deficiency syndrome of complementation group B. Hum. Mol. Genet. *7*, 1399–1405.

Rachubinski, R. A., Fujiki, Y., Mortensen, R. M., and Lazarow, P. B. (1984). Acyl-Coa oxidase and hydratase-dehydrogenase, two enzymes of the peroxisomal beta-oxidation system, are synthesized on free polysomes of clofibrate-treated rat liver. J. Cell Biol. *99*, 2241–2246.

Rospert, S., Muller, S., Schatz, G., and Glick, B. S. (1994). Fusion proteins containing the cytochrome b2 presequence are sorted to the mitochondrial intermembrane space independently of hsp60. J. Biol. Chem. *269*, 17279–17288.

Rottensteiner, H., Kramer, A., Lorenzen, S., Stein, K., Landgraf, C., Volkmer-Engert, R., and Erdmann, R. (2004). Peroxisomal membrane proteins contain common Pex19p-binding sites that are an integral part of their targeting signals. Mol. Biol. Cell *15*, 3406–3417.

Schlüter, A., Fourcade, S., Domenech-Estevez, E., Gabaldon, T., Huerta-Cepas, J., Berthommier, G., Ripp, R., Wanders, R. J., Poch, O., and Pujol, A. (2007). PeroxisomeDB: a database for the peroxisomal proteome, functional genomics and disease. Nucleic Acids Res. *35*, D815–D822.

Schuldiner, M., Metz, J., Schmid, V., Denic, V., Rakwalska, M., Schmitt, H. D., Schwappach, B., and Weissman, J. S. (2008). The GET complex mediates insertion of tail-anchored proteins into the ER membrane. Cell *134*, 634–645.

Steel, G. J., Brownsword, J., and Stirling, C. J. (2002). Tail-anchored protein insertion into yeast ER requires a novel posttranslational mechanism which is independent of the SEC machinery. Biochemistry *41*, 11914–11920.

Stefanovic, S., and Hegde, R. S. (2007). Identification of a targeting factor for posttranslational membrane protein insertion into the ER. Cell *128*, 1147–1159.

Subramani, S. (1998). Components involved in peroxisome import, biogenesis, proliferation, turnover, and movement. Physiol. Rev. *78*, 171–188.

Swinkels, B. W., Gould, S. J., and Subramani, S. (1992). Targeting efficiencies of various permutations of the consensus C-terminal tripeptide peroxisomal targeting signal. FEBS Lett. *305*, 133–136.

Tabak, H. F., Hoepfner, D., van der Zand, A., Geuze, H. J., Braakman, I., and Huynen, M. A. (2006). Formation of peroxisomes: present and past. Biochim. Biophys. Acta *1763*, 1647–1654.

Tabak, H. F., Murk, J. L., Braakman, I., and Geuze, H. J. (2003). Peroxisomes start their life in the endoplasmic reticulum. Traffic *4*, 512–518.

Tam, Y. Y., Fagarasanu, A., Fagarasanu, M., and Rachubinski, R. A. (2005). Pex3p initiates the formation of a preperoxisomal compartment from a subdomain of the endoplasmic reticulum in *Saccharomyces cerevisiae*. J. Biol. Chem. *280*, 34933–34939.

Titorenko, V. I., and Rachubinski, R. A. (1998). Mutants of the yeast *Yarrowia lipolytica* defective in protein exit from the endoplasmic reticulum are also defective in peroxisome biogenesis. Mol. Cell Biol. *18*, 2789–2803.

Tsukamoto, T., Yokota, S., and Fujiki, Y. (1990). Isolation and characterization of Chinese hamster ovary cell mutants defective in assembly of peroxisomes. J. Cell Biol. *110*, 651–660.

Vida, T. A., and Emr, S. D. (1995). A new vital stain for visualizing vacuolar membrane dynamics and endocytosis in yeast. J. Cell Biol. *128*, 779–792.

Wach, A., Brachat, A., Pohlmann, R., and Philippsen, P. (1994). New heterologous modules for classical or PCR-based gene disruptions in *Saccharomyces cerevisiae*. Yeast *10*, 1793–1808.

Wanders, R. J. (1999). Peroxisomal disorders: clinical, biochemical, and molecular aspects. Neurochem. Res. *24*, 565–580.

Winston, F., Dollard, C., and Ricupero-Hovasse, S. L. (1995). Construction of a set of convenient *Saccharomyces cerevisiae* strains that are isogenic to S288C. Yeast *11*, 53–55.

Young, B. P., Craven, R. A., Reid, P. J., Willer, M., and Stirling, C. J. (2001). Sec63p and Kar2p are required for the translocation of SRP-dependent precursors into the yeast endoplasmic reticulum in vivo. EMBO J. *20*, 262–271.